한국지반공학회논문집 제35권 7호 2019년 7월 pp. 41 ~ 50
JOURNAL OF THE KOREAN GEOTECHNICAL SOCIETY
Vol.35, No.7, July 2019 pp. 41 ~ 50

ISSN 1229-2427 (Print)
ISSN 2288-646X (Online)
https://doi.org/10.7843/kgs.2019.35.7.41

경주 압축 벤토나이트의 압축파속도와 탄성계수 산정 연구

Evaluation on Compression Wave Velocities and Moduli of Gyeongju Compacted Bentonite

Balagosa, Jebie[1]
윤 석[2] Yoon, Seok
추 연 욱[3] Choo, Yun Wook

Abstract

Gyeongju bentonite is a buffer material primarily considered in Korea and it is highly compacted as a part of an engineered barrier system (EBS) of high-level radioactive waste repository. The compacted bentonite undergoes swelling stress by groundwater penetration and thermal stress by decay heat from a canister. Therefore, the mechanical properties of the compacted bentonite buffer material is crucial for the performance assessment of EBS. This paper aims to evaluate deformation properties of Gyeongju compacted bentonite using seismic methods. Two sets of compacted bentonite specimens were prepared having dry densities of 1.59 g/cm^3 and 1.75 g/cm^3 with water contents of 10.6% and 8.7%. Free-free resonant column tests were performed to measure constrained and unconstrained compression wave velocities. With the measured wave velocities, Young's modulus (E_{max}) and constrained modulus (M_{max}), material damping ratio (D_{min}), and Poisson's ratio at small strain were determined. As results, this paper evaluates the deformation properties of Gyeongju compacted bentonite and compares them with the results of previous researches.

요 지

국내 고준위폐기물처분장 공학적방벽(EBS)의 일부가 되는 완충재로 경주 벤토나이트가 우선적으로 고려되고 있다. 압축벤토나이트는 지하수침투로 인한 팽윤압과 처분용기에서 발산되는 열응력을 경험한다. 따라서 EBS의 성능평가를 위해서 역학적 물성의 산정이 중요하다. 본 논문은 탄성파를 이용하여 경주 압축벤토나이트의 변형특성 측정을 목표로 하였다. 두 개의 1.59g/cm^{3}와 1.75g/cm^{3}의 건조밀도를 가지는 압축벤토나이트 시편을 제작하였고, 자유단-자유단 공진주시험을 수행하여 구속압축파속도와 비구속압축파속도를 측정하였다. 측정된 압축파속도를 이용하여 미소변형에서의 탄성계수(E_{max}), 구속탄성계수(M_{max}), 감쇠비(D_{min}), 포아송비를 측정하였다. 그 결과로 경주 압축벤토나이트의 변형특성을 산정·제시하여 선행연구 결과들과 비교·분석하였다.

Keywords : Gyeongju compacted bentonite, Engineered barrier system, Wave velocity, Modulus, Damping ratio, Free-free resonant column test

1 비회원, 공주대학교 건설환경공학과 석사과정 (Graduate Student, Dept. of Civil & Environmental Engrg., Kongju National Univ.)
2 정회원, 한국원자력연구원 방사성폐기물처분연구부 선임연구원 (Member, Senior Researcher, Radioactive Waste Disposal Research Division, KAERI)
3 정회원, 공주대학교 건설환경공학부 교수 (Member, Prof., Dept. of Civil & Environmental Eng., Kongju National Univ., Tel: +82-41-521-9314, Fax: +82-41-569-0287, ywchoo@kongju.ac.kr, Corresponding author, 교신저자)

* 본 논문에 대한 토의를 원하는 회원은 2020년 1월 31일까지 그 내용을 학회로 보내주시기 바랍니다. 저자의 검토 내용과 함께 논문집에 게재하여 드립니다.

1. Introduction

Clay minerals composed of bentonite is identified as a suitable candidate for buffer materials, where bentonite is a part of the smectite group containing large amounts of montmorillonite, having a self-sealing property which is advantageous for the repository assembly phase. Compacted clays are used as insulating barriers in geotechnical and geo-environmental applications (Koch, 2002). In particular, Gyeongju bentonite is a compacted buffer material commonly produced in Korea. This highly compacted buffer material plays an important role as a part of an engineered barrier system (EBS), acts as a sealing liners of radioactive waste repository, which guarantees safe disposal of high-level waste (HLW) and protects the canister against any external mechanical impact. Moreover an EBS is composed of a disposal canister with spent fuel, a buffer material, backfill material, and a near field rock mass at depths of 500 to 1,000 m below the ground surface (Fig. 1). It also serves as a gap filling material that secures the canister in place, minimize inflow of groundwater and protection against shear behavior of neighboring rock on the deep geological repository site. Especially, the compacted bentonite buffer material undergoes swelling stress by groundwater penetration and thermal stress by decay heat from canister. In order to design the compacted bentonite endurable to these swelling and thermal stresses, the mechanical property of the compacted bentonite should be evaluated. In general, the mechanical property can be evaluated by both of static and seismic methods (Richart et al., 1970). In this study, the seismic method was used to evaluate mechanical property of compacted bentonite.

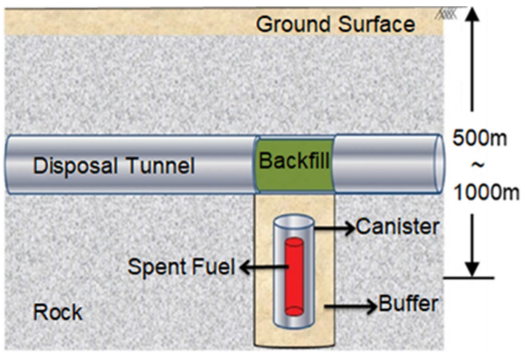

Fig. 1. Engineered Barrier System

The aim of this paper is to evaluate elastic mechanical properties of Gyeongju compacted bentonite using seismic methods. For this objective, KAERI (Korea Atomic Energy Research Institute) prepared two sets of specimens having dry densities of 1.59 g/cm^3 and 1.75 g/cm^3 with water contents of 10.6 to 8.7%. Wherein a series of free-free resonant column tests was performed to measure small-strain longitudinal unconstrained compressive wave (V_c) and constrained compressive wave (V_p) velocities, elastic modulus and damping ratio at a room temperature of 20°C. Finally, the resulting mechanical properties were compared with those collected from available literatures and discussed.

2. Testing Materials and Methods

2.1 Gyeongju Bentonite

Buffers are the materials filled in between the canister and disposal hole, which perform roles including: fixing the canister in place the disposal hole, protection against physical impacts such as those resulting from the shear behavior of rock, and minimizing groundwater inflow to prevent leakage of nuclides to nearby rock through the groundwater (Lee et al., 2007; Swedish Nuclear Fuel Supply Co./Division KBS, 1983). Bentonite, which is composed mainly of montmorillonite clay minerals, is the most suitable material for these buffers (Cho et al., 2010; Choi et al., 2008; Yoo et al., 2015). Moreover, bentonite is typically incorporated into multilevel engineered barriers, because it provides an impermeable seal between the waste packages and the surrounding host rock as it becomes progressively water saturated (Garcia-Gutierrez et al., 2001; Lloret et al., 2003; Wersin, 2003; Alonso et al., 2008; Tisato and Marelli 2013). It is known that bentonite satisfies functional criteria of the buffer (Cho et al., 1999; Yoon et al., 2019).

Gyeongju bentonite is selected for EBS material to construct Korean radioactive waste repository. In particular, Ca-type bentonite produced before 2015 in Geyongju region, Korea, is called KJ-I, and KJ-II after 2015 (Yoo et al., 2015). Ca-type bentonites (KJ-I and KJ-II) contain

montmorillonite (62~63%), feldspar (21~26%), and small amount of quartz (8~9%). X-ray diffraction (XRD) analysis results for KJ-I and KJ-II performed in the previous study are presented in Fig. 2 and Table 1. The analyses were conducted three times on each specimen, and detailed information on the material can be found in Yoon et al. (2018a). In this paper, the KJ-II powder is used in the experiment. In addition, the Gyeongju bentonite powder is classified as CH which means high plasticity based on unified soil classification system. The Atterberg limits determine liquid limit (LL) of 146.7%, plastic limit (PL) of 28.4% and plastic index (PI) of 118.3%. Furthermore, the specific gravity and surface area were 2.71 and 61.76 m^2/g (Yoon et al., 2018b).

2.2 Preparation of Compacted Bentonite

The dry density of the bentonite buffer is required to be greater than 1.6 g/cm^3 based on the Korean design guideline and the buffer should be installed as compressed blocks produced by compressing bentonite buffer powder (Yoo et al., 2015). At first, the compacted bentonite was produced by floating die method (Kim et al., 2018) with bentonite powders, and a cold isostatic pressing (CIP) technique (Kim et al., 2018) was applied in order to form a homogenous sample. Thus, two cylindrical specimens with Gyeongju bentonite were prepared, which have 1.59 g/cm^3 and 1.75 g/cm^3 of dry densities with water contents (w_c) of 10.6% and 8.7% for GJ-A and GJ-B, respectively, since the dry density of bentonite buffer is required to be greater than 1.6 g/cm^3 based on the Korean design guideline (Yoo et al., 2015). The lower dry density (1.59 g/cm^3) specimen has a preparation error with a slight insufficiency from the design guideline. The higher dry density (1.75 g/cm^3) was based on a previous full-scale field test done for another separate project (Lee et al., 2019). Thus other dry density within these two limits can be properly interpolated for future usage. The water contents of the samples as shown in Table 2, were natural water contents preserved in initial process of collecting

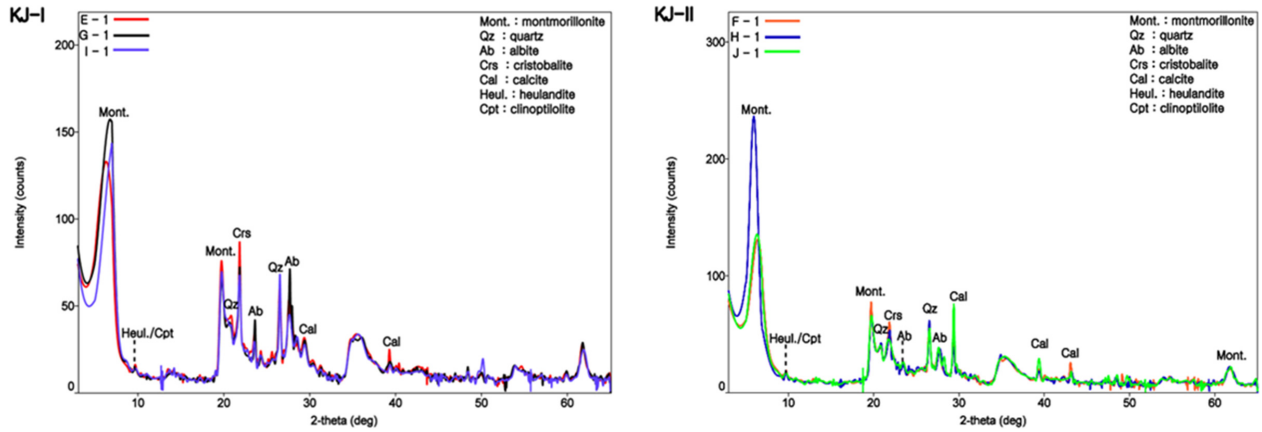

Fig. 2. X-ray diffraction patterns of the KJ-I and KJ-II powders (Yoon et al., 2018a)

Table 1. Quantitative XRD analysis for mineral constituents of KJ-I and KJ-II powders (Yoon et al., 2018a)

Bentonite type	KJ-I				KJ-II			
Sample No.	1	2	3	Avg.	4	5	6	Avg.
Montmorillonite	60.0	67.4	62.1	63.2	63.4	61.7	60.5	61.9
Albite	27.2	22.2	27.5	25.6	19.4	22.8	20.4	20.9
Quartz	5.0	4.8	5.0	4.9	5.8	4.9	5.3	5.3
Cristobalite	3.6	1.8	3.5	3.0	4.0	4.5	3.7	4.1
Calcite	2.4	2.0	2.0	2.1	4.3	3.3	6.8	4.8
Heulandite	1.8	1.7	Miner	1.8	3.0	2.7	3.3	3.0

Table 2. Properties of compacted bentonite specimens

Specimen ID	ρ_t (g/cm^3)	ρ_d (g/cm^3)	w_c (%)
GJ-A	1.76	1.59	10.6
GJ-B	1.9	1.75	8.7

* ρ_t = Total density ; ρ_d = Dry density ; W_c = Water content

bentonite, because the EBS will be constructed with natural water content at the field. Thus the water contents were not controlled to simulate actual construction conditions. The dimensions of the specimens were 50 mm in diameter and 100 mm in length.

2.3 Testing Setup and Equipment

In this study, unconstrained compression wave velocity (V_c) and constrained wave velocity (V_p) of compacted bentonite specimens were measured using free-free resonant column tests (hereafter, FFRC tests). The FFRC testing setup in this study adopts a traditional manually excited free-free method (Pucci, 2010), by applying compression waves in the specimens suspended on a fixed frame. Compression waves were created by manually hitting a ball hammer on the surface of one end as illustrated in Fig. 3. The ball hammer consists of a steel ball and a rod, and in this study the 10-mm-diameter ball was used.

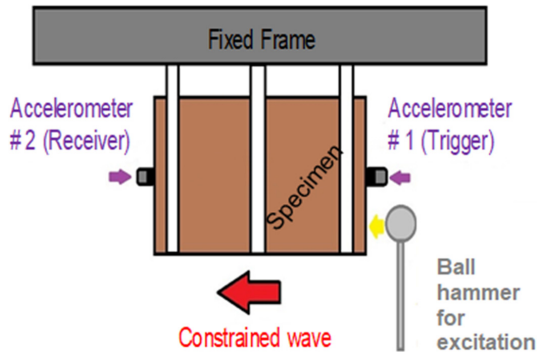

(a)

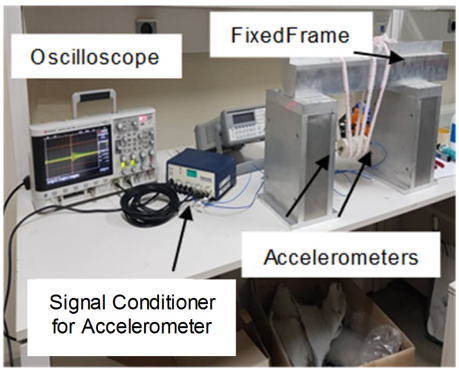

(b)

Fig. 3. Typical string-suspended specimen and manual longitudinal excitation for Vc and Vp measurements: (a) Schematic diagram, and (b) photo

The FFRC testing setup performed in this study includes: (1) accelerometers (Acc#1 and Acc#2 in Fig. 3; PCB Piezotronics 353B16, 500g pk, 1 to 10 kHz) attached on the ends of the specimen, (2) four-channel sensor signal conditioner (PCB Piezotronics 482c), (3) four channel digital oscilloscope (Infinii Vision DSO-X 2004A), and (4) a computer code using MATLAB. In order to measure the velocities, the same testing setup presented in Fig. 3 was utilized but V_c and V_p were measured by different analysis methods: frequency response curves for V_c; and direct travel-time measurement for V_p (Pucci, 2010).

2.3.1 Unconstrained Compression Wave Velocity V_c, Young's Modulus E_{max} and Material Damping Ratio D_{min}

Unconstrained compression velocity (V_c), is evaluated by peaking a longitudinal resonant frequency of the specimen. A single accelerometer attached on the receiving end (Acc#2 in Fig. 3) is utilized. Once the longitudinal source is applied on the specimen, the response signal from the Acc#2 was recorded at the oscilloscope. Then, using MATLAB functions, the fast Fourier transform (FFT) analysis was performed to obtain a typical frequency response curve as shown in Fig. 4. The resonant

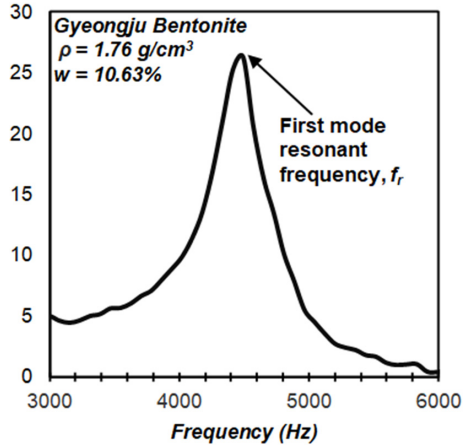

Fig. 4. Typical frequency response curve of FFRC for GJ-B

frequency f_r was determined from the frequency response curve and used to calculate unconstrained compression velocity, V_c.

Dynamic Young's Modulus of Elasticity (E_{max}) can be determined using Eq. (1) from the fundamental longitudinal resonant frequency (f_r), the length of the specimen (L) and specimen density (ρ). Dynamic Young's modulus are rapid, nondestructive and provide small-strain linear elastic moduli.

$$E_{\max} = \rho(2f_r \cdot L)^2 \quad (1)$$

Traditional static methods require the measurement of axial strain as specimen is placed under unconfined axial stress. This fractures the specimen and hence requires multiple specimens if a relationship of the change of Young's modulus with time is desired (Pucci, 2010). Under small-strain loading, the static and dynamic measured results are highly comparable for both Young's modulus of elasticity E_{max}, and Poisson's ratio v (Bay and Stokoe, 1992; Pucci, 2010; Richart et al., 1970).

Material damping ratio (D_{min}) is evaluated by the half-power bandwidth method using Eq. (2).

$$D_{\min} = \frac{f_2 - f_1}{2f_r} \quad (2)$$

where f_1 and f_2 are the half-power frequencies whose amplitude is equal to the peak resonant amplitude (A_{max}) divided by the $\sqrt{2}$ (see Fig. 5). The purpose in evaluating the resonance curve is to determine the energy loss (material damping) of waves within a material (Pucci, 2010).

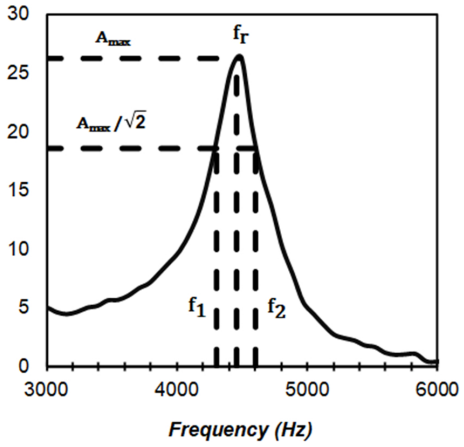

Fig. 5. Half-power bandwidth method

2.3.2 Constrained Compression V_p and Constrained Modulus M_{max}

Constrained compression velocity (V_p) is evaluated using direct travel time method (Pucci, 2010; Ezersky, 2017). The specimen is longitudinally exited at one end of the specimen and two accelerometers are attached as shown in Fig. 3. One accelerometer (Acc#1 in Fig. 3) is for the trigger source of the excitation and the other (Acc#2 in Fig. 3) is for receiving the wave travelled through the specimen. The travel time of the wave (Δt) is directly determined by comparing the trigger signal and received signal as shown in Fig. 6. After evaluating Δt, the constrained compression wave velocity (V_p), and its corresponding constrained modulus (M_{max}) were quantified.

2.3.3 Poisson's Ratio

Using the relationship of the wave velocity V_p and V_c, Poisson ratio can be determined using Eq.3 (Richart et al., 1970).

$$\upsilon = \frac{1 - \left(\frac{v_p}{v_c}\right)^2 + \sqrt[2]{\left(\left(\frac{v_p}{v_c}\right) - 1\right)^2 + 8\left(\frac{v_p}{v_c}\right)^2 \left(\left(\frac{v_p}{v_c}\right)^2 - 1\right)}}{4 \times \left(\frac{v_p}{v_c}\right)^2} \quad (3)$$

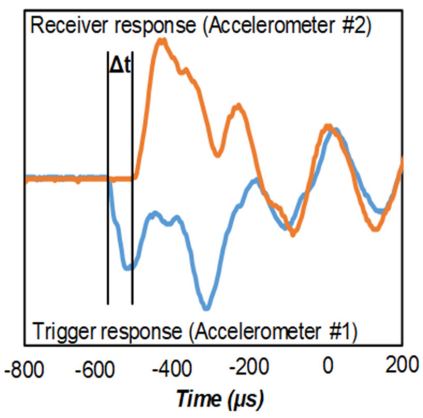

Fig. 6. Direct travel time measurement (Trial 3, using 10-mm diameter ball on GJ-A)

3. Experimental Results and Discussion

3.1 Compressive Wave Velocity

Sources of varying weights and hardness have been used by trial and error to reduce noise in the response of all types of seismic tests (Pucci, 2010). Therefore, in this study, a 10-mm-diameter steel ball was used as a manual excitation source, since it produced repeatable and cleaner responses. As a result, Fig. 7 presents comparable frequency response curves of five trials for both GJ-A and GJ-B, respectively.

Fig. 8 compares V_p and V_c of GJ-A and GJ-B to those of Tisato and Marelli (2013). The V_p of GJ-B (= 1666.67 m/s) is significantly 33% higher than that of GJ-A (= 1,250.0 m/s), due to a higher dry density of GJ-B. Moreover, the V_p of GJ-A for ρ_d = 1.59 g/cm^3 is 13.6% higher than the V_p of Tiasto and Marelli (2013) at w_c = 10% and T = 30°C. Tisato and Marelli (2013)'s examined Spanish Bentonite which is the same material as described

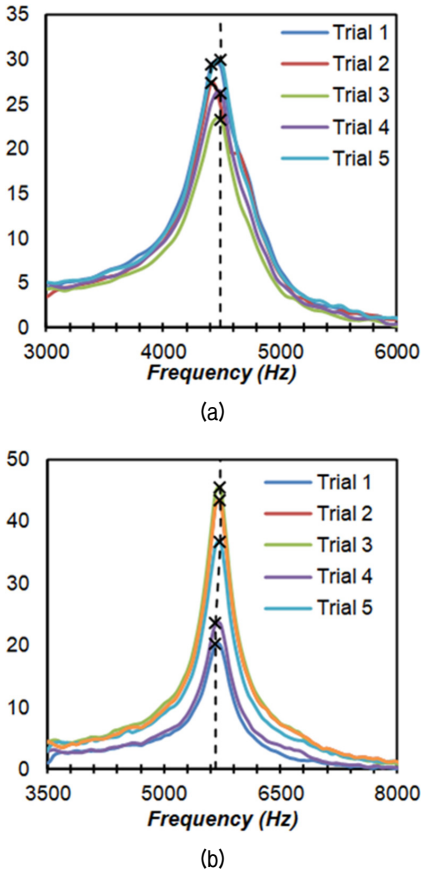

Fig. 7. Frequency response curves of (a) GJ-A, and (b) GJ-B

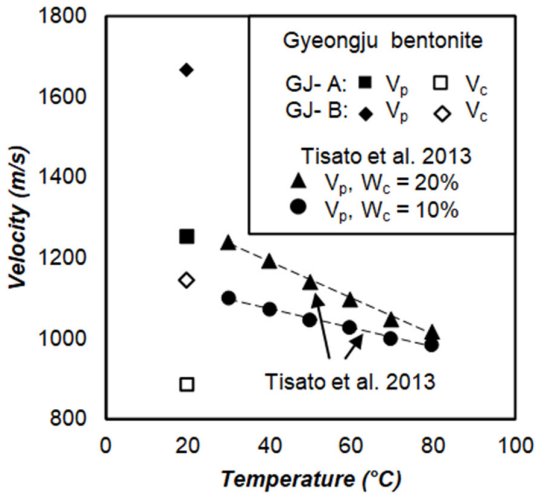

Fig. 8. Velocity measurements, compared to Spanish Bentonite with minor sandy size filler constituents montmorillonite > 95 volume %, ρ_d = 1.66 g/cm^3 ; V_p evaluation of Tisato and Marelli. (2013)

by Lloret et al. (2003), wherein V_p was measured for specimens with a dry density (ρ_d) of 1.66 g/cm^3 and w_c = 10% and 20% in the range of 30°C to 80°C. In the comparison of material matrix between KJ-II (present study) and Spanish bentonite (Tisato and Marelli, 2013), the feldspar and quartz constituents of KJ-II were higher than those of the Spanish bentonite; but the montmorillonite constituents are lower than that of the Spanish bentonite. It has been noted that with the increase in feldspar constituents in rocks, V_p increase, whereas the presence of mica decrease the compression wave velocity by Sharma et al. (2011).

The unconstrained compression velocities V_c of GJ-A and GJ-B are lower than the V_p because of its wave characteristics. In general, the fastest stress wave in any geologic medium is the constrained compression wave V_p, which can be induced with a transient impulse parallel to the direction of wave propagation (Pucci, 2010).

3.2 Young's Modulus E_{max} and Constrained Modulus M_{max}

Fig. 9 and Table 3 compare the E_{max} and M_{max} of GJ-A and GJ-B to Young's modulus of Kunigel VI, MX-80 and KJ-I reported by Cho et al. (1999). All the results clearly present the increasing trend with the increase in dry density but GJ-A and GJ-B in this study are

Table 3. Young's modulus of compacted bentonite

Compacted Bentonite	ρ_d (g/cm^3)	w_c %	E or E_{max} (GPa)	Testing Types	Ref
GJ-A (KJ-II)	1.59	10.63	1.37	FFRC	Present study
GJ-B (KJ-II)	1.75	8.69	2.49	FFRC	Present study
Kunigel VI	1.4	10	0.066	UC	Cho et al., 1999
Kunigel VI	1.5	10	0.121	UC	Cho et al., 1999
Kunigel VI	1.6	10	0.179	UC	Cho et al., 1999
Kunigel VI	1.7	10	0.257	UC	Cho et al., 1999
Kunigel VI	1.7	10	0.264	UC	Cho et al., 1999
Kunigel VI	1.8	10	0.315	UC	Cho et al., 1999
Kunigel VI	1.8	10	0.307	UC	Cho et al., 1999
MX-80	1.8	10	0.321	UC	Cho et al., 1999
MX-80	1.8	10	0.269	UC	Cho et al., 1999
Gyeongju (KJ-I)	1.4	17	0.059	UC	Cho et al., 1999
Gyeongju (KJ-I)	1.6	17	0.784	UC	Cho et al., 1999
Gyeongju (KJ-I)	1.6	17	0.588	UC	Cho et al., 1999
Gyeongju (KJ-I)	1.8	17	1.079	UC	Cho et al., 1999
Gyeongju (KJ-I)	1.8	17	1.275	UC	Cho et al., 1999

* FFRC = Free-free resonant column test ; UC = Unconfined compressive test

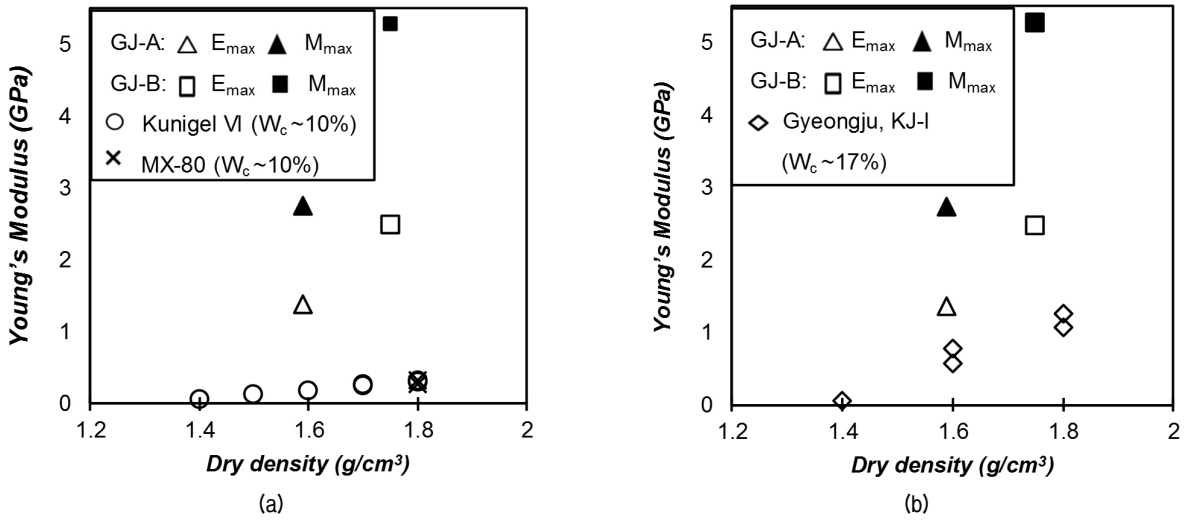

Fig. 9. Comparison with Young's Modulus of (a) Kunigel VI & MX-80, and (b) KJ-I of Cho et al. (1999)

significantly higher than the other previous results. There was a difference of 95% between GJ-B (that is, KJ-II) and KJ-I (1.8 g/cm^3) because they were tested by two different testing methods based on different strain ranges. The FFRC tests in this study measured moduli at small strain (less than 0.001%), on the other hand the previous results were done by unconfined compressive tests measuring modulus at intermediate to high strain range from 0.1% to 1%. The moduli at small strain generally present the maximum modulus (Kim and Choo, 2001; Pucci, 2010). On top of that, the high V_p measurements produce the higher value for M_{max} than E_{max}.

3.3 Material Damping Ratio D_{min}

Fig. 10 compares the D_{min} of Geongju compacted bentonite (GJ-A and GJ-B) to damping ratio at small shear strain (γ_c = 0.01%) collected from different laboratories by Vucetic and Dobry (1991) and D_{min} of the Korean compacted residual soils of Kim and Choo (2001). It was found that the damping ratios of both KJ-II materials (GJ-A and GJ-B) correspond with the relationship between

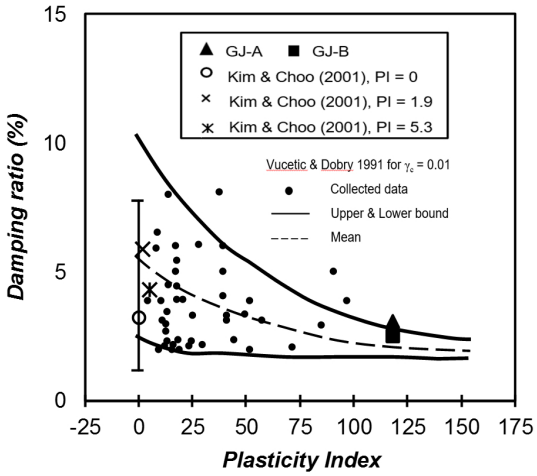

Fig. 10. Comparison with damping ratio of Vucetic & Dobry (1991) and Kim and Choo (2001)

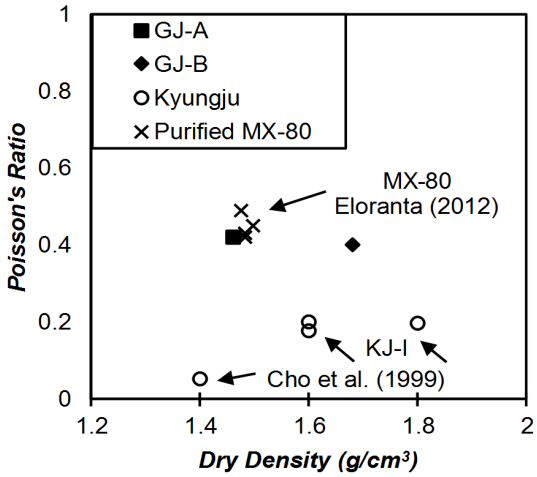

Fig. 11. Comparison with Poisson's ratio of this study with Cho et al. (1999) and Eloranta (2012)

damping ratio and PI, which the damping ratio decreases with the increase in PI. The results of this study are located at the upper boundary of Vucetic and Dobry (1991). In addition, the D_{min} of GJ-B is a little lower than that of GJ-A, indicating the denser compacted bentonite becomes more brittle. A significant decrease of 69% in D_{min} of GJ-B compared with that of the compacted residual soils with PI = 5.3 from Kim and Choo (2001) was found; and also indicating that high plastic material property of GJ-B shows a decrease of 27%, compared with the mean D_{min} of compacted residual soils from Kim and Choo (2001).

3.4 Poisson's Ratio

Fig. 11 and Table 4 present the Poisson's ratios of GJ-A and GJ-B were compared to the Poisson's ratios measured by Cho et al. (1999) and Eloranta (2012). The Poisson's ratios of GJ-A and GJ-B are comparable indicating negligible effect of dry densities; while those of KJ-1 (Cho et al., 1999) increases with the increase in dry density. However, the Poisson's ratios of Cho et al. (1999) reaches a plateau in a range of 1.6 g/cm^3 and 1.8 g/cm^3 of dry densities. The Poisson's ratio measured in this study using compressive wave velocities are higher than those of the previous results using unconfined compressive tests. In particular, Pucci (2010) reported that the Poisson's ratio measured with the ratio of V_p/V_c is higher than the other methods with V_p/V_s and V_c/V_s (here, V_p = constrained compression velocity, V_c = unconstrained compression velocity, V_s = shear wave velocity). Moreover, this discrepancy increases with lower confining pressure.

Table 4. Poisson's ratio of compacted bentonite

Compacted Bentonite	ρ_d (g/cm^3)	w_c %	Poisson's ratio	Types of Tests	Ref
GJ-A (KJ-II)	1.59	10.63	0.42	FFRC	Present study
GJ-B (KJ-II)	1.75	8.69	0.40	FFRC	Present Study
Gyeongju (KJ-I)	1.40	17.00	0.05	UC	Cho et al., 1999
Gyeongju (KJ-I)	1.60	17.00	0.18	UC	Cho et al., 1999
Gyeongju (KJ-I)	1.60	17.00	0.2	UC	Cho et al., 1999
Gyeongju (KJ-I)	1.80	17.00	0.2	UC	Cho et al., 1999
Purified MX-80	1.474	12.4	0.49	ODCT & HCT	Eloranta, 2012
Purified MX-80	1.482	7.6	0.42	ODCT & HCT	Eloranta, 2012
Purified MX-80	1.482	7.6	0.43	ODCT & HCT	Eloranta, 2012
Purified MX-80	1.497	7.6	0.45	ODCT & HCT	Eloranta, 2012

* FFRC = free-free resonant column test ; UC = Unconfined compressive test
* ODCT = One dimensional compression test ; HCT = Hydrostatic compression test

Eloranta (2012) performed one-dimensional and hydrostatic compression tests on purified MX-80 bentonite and reported that the Poisson's ratio estimated from constrained modulus and bulk modulus ranges 0.42 to 0.5 at the dry density higher than 1.47 g/cm^3. The Poisson's ratio of this study is well agreed with the previous results of Eloranta (2012) and Pucci (2010), indicating the Poisson's ratio's measured in this study are relevant for the buffer material of EBS, which is supposed to be subjected to highly constrained boundary conditions.

4. Conclusions

In this study, the seismic elastic mechanical properties of Gyeongju compacted bentonite (KJ-II) were evaluated using free-free resonant column tests. Two sets of compacted bentonite specimens were prepared having dry densities of 1.59 and 1.75 g/cm^3 with water contents of 10.6% and 8.7%. Free-free resonant column tests were performed to measure constrained and unconstrained compression wave velocities. With the measured wave velocities, Young's modulus (E_{max}) and constrained modulus (M_{max}), material damping ratio (D_{min}), and Poisson's ratio at small strain were determined and summarized in Table 5.

The V_p of GJ-A (KJ-II) is significantly higher than that of the Spanish bentonite measured by Tisato and Marelli (2013) due to its material matrix and room condition testing; and also the mineral constituents such as bentonite and feldspar, increase the rigidity of the specimen resulting to a stiffer material composite (Ismail and Shaari, 2010; Sarifuddin and Ismail, 2013). Thus Gyeongju bentonite has better mechanical characteristics to resist adverse and severe stresses applied on EBS than Spanish bentonite. For elastic moduli, a large difference between KJ-II of this study and KJ-I reported by Cho et al. (1999) was seen due to different testing methods and strain ranges. The study measures the Poisson's ratio using the seismic method at small strain (<0.001%). On the other hand Cho et al. (1999) used unconfined compressive tests usually tested at high strain range (0.1% to 1%). The present findings confirm that the D_{min} of KJ-II materials were located at the upper boundary of Vucetic and Dobry (1991), following the relationship of damping ratio and PI. In addition, the results for the Poisson's ratio of (KJ-II) are almost constant in the range of 1.59 to 1.75 g/cm^3 of dry densities. On top of that, the Poisson's ratio of this study (KJ-II) are higher than those of KJ-I tested by Cho et al. (1999) because of different testing methods and strain ranges, which is the same reason for the elastic modulus.

This study provides the first observation on dynamic elastic property of the Gyeongju compacted bentonite. The dynamic and static elastic parameters are correlated with each other, so that the results of this study will be a basis to understand the mechanical characteristics of Gyeongju compacted bentonite. However, the dynamic property may not be thoroughly representative of mechanical property. In view of this, further comparative studies between static and dynamic moduli on Gyeongju bentonite are underway. It is intended to present these test results to provide further insights on this issue in the future.

Acknowledgements

This research was supported by Basic Science Research Program (2017R1D1A3B04027989) and Nuclear Research Development Program (NRF-2017M2A8A5014857) through the National Research Foundation of Korea (NRF) funded by the Ministry of Education.

References

1. Alonso, E.E., Springman, S.M., and Ng, C.W.W. (2008), "Monitoring Large-Scale Tests for Nuclear Waste Disposal", *Geotechnical and*

Table 5. Summary of the compressive seismic velocities and moduli of this study

Sample	V_c (m/s)	V_p (m/s)	D_{min}	E_{max} (Gpa)	M_{max} (Gpa)	Poisson's ratio
GJ-A	883.00	1250.00	0.0306	1.37	2.75	0.42
GJ-B	1144.40	1666.67	0.0253	2.49	5.28	0.40

Geological Engineering, Vol.26, No.6, pp.817-826.
2. Bay, J. A. and Stokoe, I. I. (1992), "Field and laboratory determination of elastic properties of portland cement concrete using seismic techniques", *Transportation Research Record*, No.1355, pp.67-74.
3. Cho, W.J., Lee, J.O., and Kwon, S. (2010), "Analysis of thermo-hydro-mechanical process in the engineered barrier system of a high-level waste repository", *Nuclear Engineering and Design*, Vol.240, No.6, pp.1688-1698.
4. Cho, W.J., Lee, J.O., Kang, C.H., and Chun, K.S. (1999), Physicochemical, mineralogical and mechanical properties of domestic bentonite and bentonite-sand mixture as a buffer material in the high-level waste repository, *Research Report*, KAERI/TR--1388/99, Korea Atomic Energy Research Institute, Korea.
5. Choi, H.J., Lee, J.Y., and Kim, S.S. (2008), Korean reference HLW disposal system, Research Report, KAERI/TR--3563/2008, Korea Atomic Energy Research Institute, Korea.
6. Eloranta, A. (2012), *Experimental Methods for Measuring Elasto-Plastic Parameters of Bentonite Clay*, MS Dissertation, University of Jyväskylä, FIN.
7. Ezersky, M.G. (2017), "Behavior of Seismicacoustic Parameters during Deforming and Failure of Rock Samples, Large Blocks and Underground Opening: base for Monitoring", *International Journal of Geo-Engineering*, Vol.8, No.13.
8. Garcıa-Gutiérrez, M., Missana, T., Mingarro, M., Samper, J., Dai, Z., and Molinero, J. (2001), "Solute Transport Properties of Compacted Ca-Bentonite used in FEBEX Project", *Journal of Contaminant Hydrology*, Vol.47, No.2-4, pp.127-137.
9. Ismail, H. and Shaari, S.M. (2010), "Curing characteristics, tensile properties and morphology of palm ash or halloysite nanotubes or ethylene-propylene-diene monomer (EPDM) hybrid composites", *Polymer Testing*, Vol.29, No.7, pp.872-878.
10. Kim, D.S. and Choo, Y.W. (2001), "Dynamic deformation characteristics of cohesionless soils in korea using resonant column tests", *Journal of Korean Geotechnical Society*, Vol.17, No.5, pp.115-128.
11. Kim, J.S., Yoon, S., Cho, W.J., Choi, Y.C., and Kim, G.Y. (2018), "A Study on the Manufacturing Characteristics and Field Applicability of Engineering-scale Bentonite Block in a High-level Nuclear Waste Repository", *Journal of Nuclear Fuel Cycle and Waste Technology*, Vol.16, No.1, pp.123-136.
12. Koch, D. (2002), "Bentonites as a Basic Material for Technical base Liners and Site Encapsulation Cut-off Walls", *Applied Clay Science*, Vol.21, No.1-2, pp.1-11.
13. Lee, C., Yoon, S., Cho, W.J., Jo, Y., Lee, S., Jeon, S., and Kim, G.Y. (2019), "Study on Thermal, Hydraulic, and Mechanical Properties of KURT Granite and Geyongju Bentonite", *Journal of Nuclear Fuel Cycle and Waste Technology*, Vol.17, No.S, pp.81-95.
14. Lee, J., Cho, D., Choi, H., and Choi, J. (2007), "Concept of a Korean Reference Disposal System for Spent Fuels", *Journal of Nuclear Science and Technology*, Vol. 44, No.12, pp.1565-1573.
15. Lloret, A., Villar, M.V., Sanchez, M., Gens, A., Pintado, X., and Alonso, E. (2003), "Mechanical behaviour of Heavily Compacted Bentonite under High Suction Changes", *Geotechnique*, Vol.53, No.1, pp.27-40.
16. Pucci, M.J. (2010), *Development of a Multi-measurement Confined Free-Free Resonant Column Device and Initial Studies*, Ph.D Dissertation, University of Texas at Austin, TX.
17. Richart, F.E. Hall, J.R., and Woods R.D. (1970), *Vibrations of Soils and Foundations*, Prentice-Hall. Inc., Englewood Cliffs, New Jersey.
18. Sarifuddin, N. and Ismail, H. (2013), "Comparative study on the effect of bentonite or feldspar filled low-density polyethylene or thermoplastic sago starch or kenaf core fiber composites", *Bio-resources*, Vol.8, No.3, pp.4238-4257.
19. Sharma, R., Gupta, V., Arora, B. R., and Sen, K. (2011), "Petrophysical properties of the Himalayan granitoids: implication on composition and source", *Tectonophysics*, Vol.497, No.1-4, pp. 23-33.
20. Swedish Nuclear Fuel Supply Co./Division KBS (1983), Final storage of spent nuclear fuel-KBS-3, III barriers, Technical Report, pp.9:1-16:12.
21. Tisato, N. and Marelli, S. (2013), "Laboratory Measurements of the Longitudinal and Transverse Wave Velocities of Compacted Bentonite as a Function of Water Content, Temperature, and Confining Pressure", *Journal of Geophysical Research: Solid Earth*, Vol.118, No.7, pp.3380-3393.
22. Vucetic, M. and Dobry, R. (1991), "Effect of Soil Plasticity on Cyclic Response", *Journal of Geotechnical Engineering*, Vol.117, No.1, pp.89-107.
23. Wersin, P. (2003), "Geochemical Modelling of Bentonite Porewater in High-level Waste Repositories", *Journal of Contaminant Hydrology*, Vol.61, No.1-4, pp.405-422.
24. Yoo, M., Choi, H.J., Lee, M.S., and Lee, S.Y. (2015), Chemical and Mineralogical Characterization of Domestic Bentonite for a Buffer of an HLW Repository, *Research Report,* KAERI/TR-6182, Korean Atomic Energy Research Institute.
25. Yoon, S., Cho, W., Lee, C., and Kim, G.Y. (2018a), "Thermal Conductivity of Korean Compacted Bentonite Buffer Materials for a Nuclear Waste Repository", *Energies*, Vol.11, No.9, p.2269.
26. Yoon, S., Kim, M.J., Lee, S.R., and Kim, G.Y. (2018b), "Thermal Conductivity Estimation of Compacted Bentonite Buffer Materials for a High-level Radioactive Waste Repository", *Nuclear Technology*, Vol.204, No.2, pp.213-226.
27. Yoon, S., Jeon, J.S., Kim, G.Y., Seong, J.H., and Baik, M.H. (2019), "Specific Heat Capacity Model for Compacted Bentonite Buffer Materials", *Annals of Nuclear Energy*, Vol.125, pp.18-25.

Received : May 26th, 2019
Revised : June 9th, 2019
Accepted : June 11th, 2019